2017 American Control Conference
Sheraton Seattle Hotel
May 24–26, 2017, Seattle, USA

Discrete-time distributed Kalman filter design for multi-vehicle systems

Daniel Viegas, Pedro Batista, Paulo Oliveira, and Carlos Silvestre

Abstract— **This paper addresses the problem of distributed state estimation in a multi-vehicle framework. In the scenario envisioned in this work, each vehicle aims to estimate its own state by implementing a local state observer which relies on locally available measurements and limited communication with other vehicles in the vicinity. The dynamics of the problem are formulated as a more general discrete-time Kalman filtering problem with a sparsity constraint on the gain and, based on this formulation, a method for computation of steady-state observer gains for arbitrary fixed measurement topologies is introduced. The proposed method consists in the optimization of the time-varying distributed Kalman filter over a finite time window to approximate steady-state behavior and compute well-performing steady-state observer gains. To assess the performance of the proposed solution, simulation results are detailed for the practical case of a formation of Autonomous Underwater Vehicles (AUVs).**

I. Introduction

Advances in science and technology in the last decades have led to an interest in using multiple autonomous vehicles cooperatively to solve problems in a more time and resource efficient way, or even perform tasks beyond the capabilities of a single vehicle. In fact, the use of autonomous vehicles in formations offers attractive possibilities in areas as diverse as unmanned formation flight [7], automated highways systems [3], and underwater applications [8], [5].

The use of multi-agent systems has led to new challenges in the field of control and estimation. While the use of centralized solutions is attractive as the underlying theory is well understood, it may lead to severe problems during implementation due to the reliance on a central processing node. As the number of vehicles increases, the computational load on the central node and the number of communications needed will also increase, and may in fact render the centralized solution inviable. On the other hand, using distributed solutions can help bypass these scaling problems. However, there is a trade-off: while implementation is simple and efficient, design and analysis become much more complex. Regarding distributed state estimation, interesting approaches can be found in works such as [15], [19], [11], and [9]. The closely related area of distributed control has also seen a wealth of contributions, such as those in [16], [13], and [12]. For more general works on this subject, see e.g. [10], [14].

This paper addresses the problem of distributed state estimation for formations of autonomous vehicles in a discrete-time framework, in which each vehicle in the formation aims to estimate its own state based on locally available measurements and communication with other vehicles in the vicinity. It is assumed that one or a few vehicles have access to measurements of their own state, while the rest must rely on measurements of their state relative to one or more other vehicles in the vicinity, as well as updated state estimates received from those vehicles through communication. In previous work by the authors in [17] and [18], Linear Matrix Inequality (LMI) theory was used to derive algorithms to design distributed state observers. In this paper, we consider another approach based on the discrete-time Kalman filter equations to design a computationally efficient solution to obtain gains for the distributed state observer. The problem is reformulated as the more general problem of Kalman filtering with a sparsity constraint on the gain, and a method to compute distributed observer gains is introduced, which consists in an iterative algorithm that optimizes the observer gains over a finite-time window to approximate optimal steady-state behavior. While the solution in [17] requires solving an optimization problem numerically in each step, in the method proposed here the solution of the optimization problem solved in each iteration can be obtained in closed form. This framework is then particularized to a formation of Autonomous Underwater Vehicles (AUVs), and an equivalent continuous-discrete formulation for local observer design is introduced to take advantage of the much faster sampling rate of on-board instrumentation in comparison with the positioning system. Finally, the performance of the proposed solution is assessed in simulation.

The rest of the paper is organized as follows. Section II details the structure of the local state observers, and Section III describes the more general problem of sparse Kalman filtering. Section IV introduces the finite-horizon method for computing gains for distributed state observers, and Section V details simulation results for a formation of AUVs. Finally, Section VI summarizes the main conclusions of the paper.

A. Notation

A block diagonal matrix $\mathbf{A}$ with n blocks $\mathbf{A}_1, \mathbf{A}_2, \ldots, \mathbf{A}_n$ is denoted by $\mathbf{A} = \text{diag}(\mathbf{A}_1, \mathbf{A}_2, \ldots, \mathbf{A}_n)$. The notation $\text{vec}(\cdot)$ denotes the vectorizing operator. $\mathbf{P} \succ \mathbf{0}$ indicates that the symmetric matrix $\mathbf{P}$ is positive definite. The Kronecker product of two matrices $\mathbf{A}$ and $\mathbf{B}$ is denoted by $\mathbf{A} \otimes \mathbf{B}$.

This work was supported by the Macao Science & Technology Development Fund (FDCT) through Grant FDCT/065/2014/A, by project MYRG2015-00127-FST of the University of Macau, and by the Fundação para a Ciência e a Tecnologia (FCT) through ISR under contract LARSyS FCT [UID/EEA/50009/2013] and through IDMEC, under contract LAETA FCT [UID/EMS/50022/2013]. The work of D. Viegas was partially supported by the Ph.D. Student Scholarship SFRH/BD/71486/2010, from FCT.

D. Viegas and C. Silvestre are with the Department of Electrical and Computer Engineering of the Faculty of Science and Technology of the University of Macau, Macao, China. P. Batista is with the Institute for Systems and Robotics (ISR), Instituto Superior Técnico, Universidade de Lisboa, Lisboa, Portugal. P. Oliveira is with ISR and IDMEC, Instituto Superior Técnico, Universidade de Lisboa, Lisboa, Portugal. C. Silvestre is on leave from Instituto Superior Técnico/University of Lisbon, 1049-001 Lisbon, Portugal. dviegas@isr.ist.utl.pt, pbatista@isr.tecnico.ulisboa.pt, pjcro@isr.ist.utl.pt, csilvestre@umac.mo

II. Problem statement

Consider a formation composed of N autonomous vehicles, each indexed by a distinct integer i. The problem considered in this paper is the design of a distributed state estimation solution such that each vehicle can estimate its own state using only measurements obtained from sensors mounted on-board and limited communication with other vehicles. The measurements available to each vehicle are divided into two categories: one or more vehicles have access to measurements of their own state, referred to as *inertial* measurements in the sequel, while the rest must rely instead on measurements of their state *relative* to other vehicles in the vicinity. For the latter case, it is also assumed that they receive state estimates from the corresponding vehicles through communication. The solution proposed here consists in the implementation of a local state observer on-board each vehicle, which uses the aforementioned locally available measurements and communication to estimate the state of the vehicle in real time.

Vehicle formations such as the one considered in this paper can be compactly described by directed graphs. A directed graph, or digraph, $\mathcal{G} := (\mathcal{V}, \mathcal{E})$ is composed of a set $\mathcal{V}$ of vertices together with a set of directed edges $\mathcal{E}$, which are ordered pairs of vertices. Such an edge can be expressed as $e = (a, b)$, meaning that edge e is incident on vertices a and b, directed towards b. For a vertex i, its in-degree ν_i is the number of edges directed towards and incident on it, and its in-neighborhood $\mathcal{D}_i = \{d_i^1, d_i^2, \ldots, d_i^{\nu_i}\}$ is the set of corresponding vertices. A digraph $\mathcal{G}$ with n_v vertices and n_e edges can be described by an incidence matrix $\boldsymbol{\mathcal{I}}_{\mathcal{G}} \in \mathbb{R}^{n_v \times n_e}$, whose individual entries follow

$$[\boldsymbol{\mathcal{I}}_{\mathcal{G}}]_{jk} = \begin{cases} 1, & \text{edge } k \text{ directed towards } j \\ -1, & \text{edge } k \text{ directed away from } j \\ 0, & \text{edge } k \text{ not incident on } j \end{cases}.$$

Consider the vehicle formation described at the beginning of this section. Its measurement topology can be described by a digraph $\mathcal{G}_M$, in which each vertex represents a distinct vehicle, and an edge (a, b) signifies that vehicle b has access to a measurement relative to vehicle a. Finally, define a special set of edges of the form $(0, i)$, connected to only one vertex, which represent the inertial measurements available to some of the vehicles.

A. Local state observers

For a vehicle i with inertial measurements, its dynamics are described by the Linear Time-Invariant (LTI) system

$$\begin{cases} \mathbf{x}_i(k+1) = \mathbf{A}_L \mathbf{x}_i(k) + \mathbf{B}_L \mathbf{u}_i(k) + \mathbf{w}_i(k) \\ \mathbf{y}_i(k) = \mathbf{C}_L \mathbf{x}_i(k) + \mathbf{v}_i(k) \end{cases}, \quad (1)$$

where $\mathbf{x}_i(k) \in \mathbb{R}^{n_L}$ is the state of vehicle i, to be estimated, $\mathbf{u}_i(k) \in \mathbb{R}^{m_L}$ is the input of the system, and $\mathbf{y}_i(k) \in \mathbb{R}^{o_L}$ is the measured output at time k. $\mathbf{A}_L$, $\mathbf{B}_L$, and $\mathbf{C}_L$ are given constant matrices of appropriate dimensions. $\mathbf{w}_i(k) \in \mathbb{R}^{n_L}$ and $\mathbf{v}_i(k) \in \mathbb{R}^{o_L}$ represent process and observation noise, and are assumed to be zero-mean white Gaussian processes with associated covariance matrices $\mathbf{Q}_i \succeq \mathbf{0} \in \mathbb{R}^{n_L \times n_L}$ and $\mathbf{R}_i \succ \mathbf{0} \in \mathbb{R}^{o_L \times o_L}$, respectively. It is assumed that the pair $(\mathbf{A}_L, \mathbf{C}_L)$ is observable. To estimate the state, we adopt a prediction-filtering scheme similar to the one used in the Kalman filter. Denote the predicted state estimate at time k by $\hat{\mathbf{x}}_i(k|k-1) \in \mathbb{R}^{n_L}$ and the filtered state estimate by $\hat{\mathbf{x}}_i(k|k) \in \mathbb{R}^{n_L}$. The predicted estimate is updated following

$$\hat{\mathbf{x}}_i(k+1|k) = \mathbf{A}_L \hat{\mathbf{x}}_i(k|k) + \mathbf{B}_L \mathbf{u}_i(k), \quad (2)$$

and the filtered estimate follows

$$\hat{\mathbf{x}}_i(k+1|k+1) = \hat{\mathbf{x}}_i(k+1|k) + \mathbf{K}_i(\mathbf{y}_i(k+1) - \mathbf{C}_L \hat{\mathbf{x}}_i(k+1|k)), \quad (3)$$

in which $\mathbf{K}_i \in \mathbb{R}^{n_L \times o_L}$ is a constant matrix of output injection gains. For this case, it is straightforward to compute gains such that the observer features globally exponentially stable error dynamics, see e.g. [1].

On the other hand, if vehicle i has access to relative measurements to other vehicles in the formation, its dynamics follow

$$\begin{cases} \mathbf{x}_i(k+1) = \mathbf{A}_L \mathbf{x}_i(k) + \mathbf{B}_L \mathbf{u}_i(k) + \mathbf{w}_i(k) \\ \mathbf{y}_i(k) = \mathbf{C}_i \Delta\mathbf{x}_i(k) + \mathbf{v}_i(k) \end{cases},$$

in which $\mathbf{y}_i(k) \in \mathbb{R}^{o_L \nu_i}$, $\mathbf{C}_i = \mathbf{I}_{\nu_i} \otimes \mathbf{C}_L$, and

$$\Delta\mathbf{x}_i(k) := \begin{bmatrix} \mathbf{x}_i(k) - \mathbf{x}_{d_i^1}(k) \\ \mathbf{x}_i(k) - \mathbf{x}_{d_i^2}(k) \\ \vdots \\ \mathbf{x}_i(k) - \mathbf{x}_{d_i^{\nu_i}}(k) \end{bmatrix} \in \mathbb{R}^{n_L \nu_i}. \quad (4)$$

The remaining variables are defined as in (1). For this case, the following prediction-filtering structure for the system (4) can be implemented. The predicted estimate is updated following (2), and the filtered estimate follows

$$\hat{\mathbf{x}}_i(k+1|k+1) = \hat{\mathbf{x}}_i(k+1|k) + \mathbf{K}_i(\mathbf{y}_i(k+1) - \mathbf{C}_i \Delta\hat{\mathbf{x}}_i(k+1|k)), \quad (5)$$

where $\mathbf{K}_i \in \mathbb{R}^{n_L \times o_L \nu_i}$ is a constant matrix of observer gains, to be computed, and $\Delta\hat{\mathbf{x}}_i(k|k-1)$ is constructed using the state estimates received through communication.

B. Global dynamics

The global dynamics of the formation can be represented by the LTI system

$$\begin{cases} \mathbf{x}(k+1) = \mathbf{A}_g \mathbf{x}(k) + \mathbf{B}_g \mathbf{u}(k) + \mathbf{w}(k) \\ \mathbf{y}(k) = \mathbf{C}_g \mathbf{x}(k) + \mathbf{v}(k) \end{cases},$$

where $\mathbf{x}(k) := \begin{bmatrix} \mathbf{x}_1^\mathsf{T}(k) & \ldots & \mathbf{x}_N^\mathsf{T}(k) \end{bmatrix}^\mathsf{T} \in \mathbb{R}^{n_L N}$ is the state of the whole formation, $\mathbf{y}(k) \in \mathbb{R}^{o_L M}$ is the concatenation of all the outputs in the formation, M being the number of edges in $\mathcal{G}_M$, and $\mathbf{u}(k) \in \mathbb{R}^{m_L N}$ is the concatenation of the inputs of each vehicle. The state and measurement noise vectors $\mathbf{w}(k) \in \mathbb{R}^{n_L N}$ and $\mathbf{v}(k) \in \mathbb{R}^{o_L M}$ are obtained in the same fashion. The matrices $\mathbf{A}_g$, $\mathbf{B}_g$, and $\mathbf{C}_g$ are built from the dynamics of the individual agents, following

$$\begin{cases} \mathbf{A}_g = \mathbf{I}_N \otimes \mathbf{A}_L \\ \mathbf{B}_g = \mathbf{I}_N \otimes \mathbf{B}_L \\ \mathbf{C}_g = \boldsymbol{\mathcal{I}}_{\mathcal{G}_M}^\mathsf{T} \otimes \mathbf{C}_L \end{cases}.$$

The local state observers can also be grouped in a similar way. The predicted state estimate $\hat{\mathbf{x}}(k|k-1) := \begin{bmatrix} \hat{\mathbf{x}}_1^\mathsf{T}(k|k-1) & \ldots & \hat{\mathbf{x}}_N^\mathsf{T}(k|k-1) \end{bmatrix}^\mathsf{T}$ is updated following

$$\hat{\mathbf{x}}(k+1|k) = \mathbf{A}_g \hat{\mathbf{x}}(k|k) + \mathbf{B}_g \mathbf{u}(k),$$

and the filtered estimate $\hat{\mathbf{x}}(k|k) := \left[\hat{\mathbf{x}}_1^\mathsf{T}(k|k) \ \dots \ \hat{\mathbf{x}}_N^\mathsf{T}(k|k)\right]^\mathsf{T}$ follows

$$\hat{\mathbf{x}}(k+1|k+1) = \hat{\mathbf{x}}(k+1|k) + \mathbf{K}_g(\mathbf{y}(k+1) - \mathbf{C}_g\hat{\mathbf{x}}(k+1|k)),$$

where $\mathbf{K}_g \in \mathbb{R}^{n_L N \times o_L M}$ is the matrix of observer gains. To account for the fact that each local observer only has access to some measurements, $\mathbf{K}_g$ must follow a block diagonal structure:

$$\mathbf{K}_g = \operatorname{diag}(\mathbf{K}_1, \mathbf{K}_2, \dots, \mathbf{K}_N). \tag{6}$$

Due to this structural constraint on the observer gain, classical observer design methods cannot be applied.

III. Kalman filter with sparsity constraints

The block diagonal structure for the observer gain in (6) belongs to a more general category of constraints, commonly denoted as sparsity constraints. For $\mathbf{E} \in \mathbb{R}^{n\times o}$, the set of matrices which follow the sparsity pattern of $\mathbf{E}$ is defined as

$$\text{Sparse}(\mathbf{E}) = \{\mathbf{K} \in \mathbb{R}^{n\times o} : [\mathbf{E}]_{ij} = 0 \implies [\mathbf{K}]_{ij} = 0, \\ i = 1, \dots, n, \ j = 1, \dots, o\}.$$

This section details the problem of Kalman filtering with sparsity constraints on the filter gain matrix.

Consider the discrete time LTI system

$$\begin{cases} \boldsymbol{x}(k+1) = \mathbf{A}\boldsymbol{x}(k) + \mathbf{B}\boldsymbol{u}(k) + \boldsymbol{w}(k) \\ \boldsymbol{y}(k) = \mathbf{C}\boldsymbol{x}(k) + \boldsymbol{v}(k) \end{cases},$$

where $\boldsymbol{x}(k) \in \mathbb{R}^n$, $\boldsymbol{u}(k) \in \mathbb{R}^m$, and $\boldsymbol{y}(k) \in \mathbb{R}^o$ are the state, input, and output of the system, respectively, $\boldsymbol{w}(k) \in \mathbb{R}^n$ and $\boldsymbol{v}(k) \in \mathbb{R}^o$ are the process and observation noises, which are assumed to be zero-mean white Gaussian processes with associated covariance matrices $\mathbf{Q} \succeq \mathbf{0} \in \mathbb{R}^{n\times n}$ and $\mathbf{R} \succ \mathbf{0} \in \mathbb{R}^{o\times o}$, respectively, and $\mathbf{A}$, $\mathbf{B}$, and $\mathbf{C}$ are given constant matrices of appropriate dimensions.

The predicted state estimate is computed following

$$\hat{\boldsymbol{x}}(k+1|k) = \mathbf{A}\hat{\boldsymbol{x}}(k|k) + \mathbf{B}\mathbf{u}(k), \tag{7}$$

and the estimation error covariance is updated accordingly:

$$\mathbf{P}(k+1|k) = \mathbf{A}\mathbf{P}(k|k)\mathbf{A}^\mathsf{T} + \mathbf{Q}. \tag{8}$$

Then, the a priori estimate (7) for $\boldsymbol{x}(k+1)$ is corrected using the observation $\boldsymbol{y}(k+1)$. The filtered state estimate is computed following

$$\hat{\boldsymbol{x}}(k+1|k+1) = \\ \hat{\boldsymbol{x}}(k+1|k) + \mathbf{K}(k+1)(\boldsymbol{y}(k+1) - \mathbf{C}\hat{\boldsymbol{x}}(k+1|k)),$$

where $\mathbf{K}(k+1) \in \mathbb{R}^{n\times o}$ is the filter gain, and the corresponding estimation error covariance is given by

$$\mathbf{P}(k+1|k+1) = \mathbf{K}(k+1)\mathbf{R}\mathbf{K}^\mathsf{T}(k+1) \\ + (\mathbf{I} - \mathbf{K}(k+1)\mathbf{C})\mathbf{P}(k+1|k)(\mathbf{I} - \mathbf{K}(k+1)\mathbf{C})^\mathsf{T}. \tag{9}$$

For a finite time window $W \in \mathbb{N}$, the problem of designing a Kalman filter subject to a sparsity constraint on the gain matrix can then be formulated as follows. Given a sparsity pattern $\mathbf{E} \in \mathbb{R}^{n\times o}$ and an initial state estimate $\hat{\boldsymbol{x}}(0|0)$ with associated error covariance $\mathbf{P}(0|0) \succ \mathbf{0}$, solve the optimization problem

$$\begin{aligned} \underset{\substack{\mathbf{K}(i)\in\mathbb{R}^{n\times o} \\ i=1,2,\dots,W}}{\text{minimize}} \quad & \sum_{k=1}^{W} \operatorname{tr}(\mathbf{P}(k|k)) \\ \text{subject to} \quad & \mathbf{K}(i) \in \text{Sparse}(\mathbf{E}), \ i = 1, 2, \dots, W \end{aligned} \tag{10}$$

TABLE I

Finite-horizon algorithm for computation of observer gains

(1)	**Initialization:** Select a window size, W, and a set of initial covariances $\mathbf{P}(k\|k)$, $k = 0, 1, \dots, W$ and observer gains $\mathbf{K}(k)$, $k = 1, \dots, W$. Select a stopping criterion, for example a minimum improvement on the objective function of (10) or a fixed number of iterations.
(2)	Set i = W.
(3)	**Inner loop:**
	(a) Fix all observer gains except for $\mathbf{K}(i)$, and solve (12) for $\mathbf{K}(i)$, replacing the previous value for that gain.
	(b) Set $i = i - 1$. If $i = 0$, exit the inner loop to Step (4). Otherwise, go to (a).
(4)	Recompute the covariances $\mathbf{P}(1\|1)$ through $\mathbf{P}(W\|W)$ using the new observer gains.
(5)	If the stopping criterion is met, stop. Otherwise, go to (2).

Now, consider that we choose a constant gain $\mathbf{K}_\infty$ for all steps instead of a sequence of gains $\mathbf{K}(k)$. Then, if $\mathbf{K}_\infty$ stabilizes the error dynamics of the filter (7)-(9), it is well known (see e.g. [1]) that the estimation error covariance converges to a steady-state solution, that is, there exists a finite constant $\mathbf{P}_\infty \in \mathbb{R}^{n\times n} \succ \mathbf{0}$ such that

$$\lim_{k\to+\infty} \mathbf{P}(k|k) = \mathbf{P}_\infty.$$

Thus, finding the optimal steady-state gain for the Kalman filter subject to a sparsity constraint can be formulated as the optimization problem

$$\begin{aligned} \underset{\mathbf{K}_\infty\in\mathbb{R}^{n\times o}}{\text{minimize}} \quad & \operatorname{tr}(\mathbf{P}_\infty) \\ \text{subject to} \quad & \mathbf{K}_\infty \in \text{Sparse}(\mathbf{E}) \end{aligned} \tag{11}$$

The optimization problems (10) and (11) are both nonconvex and, unlike the unconstrained Kalman filter, finding their optimal solution is still an open problem.

IV. Finite-horizon method for computation of observer gains

This section details a method to compute steady-state gains for a state observer subject to a sparsity constraint on the gain. This method is based on the finite-horizon problem (10). The idea behind this formulation is to approximate steady-state behavior by making W large enough, and thus obtain a constant filter gain that stabilizes the error dynamics of the state observer and offers good filtering performance.

While the optimization problem (10) is nonconvex, if all the gains are fixed to an arbitrary constant value except for a single $\mathbf{K}(k)$, the optimization problem (10) takes the form

$$\begin{aligned} \underset{\mathbf{K}(k)\in\mathbb{R}^{n\times o}}{\text{minimize}} \quad & \sum_{i=1}^{W} \operatorname{tr}(\mathbf{P}(i|i)) \\ \text{subject to} \quad & \mathbf{K}(k) \in \text{Sparse}(\mathbf{E}) \end{aligned} \tag{12}$$

which is quadratic, and can thus be solved using conventional methods. Taking advantage of this fact, we propose the algorithm detailed in Table I to compute observer gains for the Kalman filter subject to a sparsity constraint. Note that the proposed algorithm yields a time-varying gain matrix. To obtain a constant steady-state gain with the desired sparsity constraint, one can run the algorithm with a window size W large enough to recover steady-state behavior and thus approximate the optimal solution of (11). Then, from the

sequence of gains $\mathbf{K}(k),\ k = 1, 2, \ldots, W$, select the one that yields the best steady-state covariance $\mathbf{P}_\infty$, found by propagating the error covariance equations (8) and (9) for each of the gains.

Remark 1: The algorithm detailed in Table I requires a set of initial gains and error covariances to begin its execution. The simplest solution is to set all the $\mathbf{K}(k)$ to zero, although it may lead to numerical problems with unstable systems. Another solution is to initialize the algorithm with stabilizing centralized gains, as they will be replaced by gains with the desired sparsity pattern after the first outer loop iteration.

A. Closed-form solution of the partial problem

The solution of the partial problem (12) can be computed in closed form, significantly reducing the computational complexity of the algorithm detailed in Table I. To do so, define a matrix $\mathbf{Z}$ that selects the nonzero elements in $\text{vec}(\mathbf{K}(k))$ according to the desired sparsity pattern. For example, for a $\mathbf{K}(k)$ of the form

$$\mathbf{K}(k) = \begin{bmatrix} k_1 & 0 \\ k_2 & k_3 \\ 0 & k_4 \end{bmatrix},$$

then $\text{vec}(\mathbf{K}(k)) = \begin{bmatrix} k_1 & k_2 & 0 & 0 & k_3 & k_4 \end{bmatrix}^\mathsf{T}$ and

$$\mathbf{Z} = \begin{bmatrix} 1 & 0 & 0 & 0 & 0 & 0 \\ 0 & 1 & 0 & 0 & 0 & 0 \\ 0 & 0 & 0 & 0 & 1 & 0 \\ 0 & 0 & 0 & 0 & 0 & 1 \end{bmatrix}.$$

The closed-form solution of (12) can then be computed in vector form following

$$\text{vec}(\mathbf{K}(k)) = \mathbf{\Xi}(k)\,\text{vec}(\mathbf{\Lambda}(k+1)\mathbf{P}(k|k-1)\mathbf{C}^\mathsf{T}), \quad (13)$$

where

$$\mathbf{\Xi}(k) = \mathbf{Z}^\mathsf{T}\left(\mathbf{Z}(\mathbf{S}(k) \otimes \mathbf{\Lambda}(k+1))\mathbf{Z}^\mathsf{T}\right)^{-1}\mathbf{Z},$$

in which

$$\mathbf{S}(k) = \mathbf{C}\mathbf{P}(k|k-1)\mathbf{C}^\mathsf{T} + \mathbf{R}$$

and

$$\mathbf{\Lambda}(k+1) = \mathbf{I}_n + \sum_{i=k+1}^{W} \mathbf{\Gamma}^\mathsf{T}(k+1, i)\mathbf{\Gamma}(k+1, i),$$

with

$$\mathbf{\Gamma}(k_i, k_f) = \prod_{j=k_i}^{k_f} (\mathbf{I}_n - \mathbf{K}(k_i + k_f - j)\mathbf{C})\mathbf{A}.$$

When $k_i > k_f$, we follow the convention $\mathbf{\Gamma}(k_i, k_f) = \mathbf{I}_n$. The derivation of (13) is omitted due to lack of space.

V. Simulation results for a formation of AUVs

Consider a formation composed of N AUVs, and suppose that each vehicle has sensors mounted on-board which give access to either measurements of its own position in an inertial reference coordinate frame $\{I\}$, or measurements of its position relative to one or more AUVs in the vicinity, as well as updated position estimates from those vehicles.

Let $\{B_i\}$ denote the body-fixed coordinate frame associated with the i-th AUV. For a vehicle i with inertial position readings, its linear motion can be modeled by the system

$$\begin{cases} \dot{\mathbf{p}}_i(t) = \boldsymbol{\mathcal{R}}_i(t)\mathbf{s}_i(t) \\ \dot{\mathbf{s}}_i(t) = -\boldsymbol{\mathcal{S}}(\boldsymbol{\omega}_i(t))\mathbf{s}_i(t) + \mathbf{g}_i(t) + \mathbf{a}_i(t) \\ \dot{\mathbf{g}}_i(t) = -\boldsymbol{\mathcal{S}}(\boldsymbol{\omega}_i(t))\mathbf{g}_i(t) \\ \mathbf{y}_i(t) = \mathbf{p}_i(t) \end{cases},$$

where $\mathbf{p}_i(t) \in \mathbb{R}^3$ is the inertial position of the i-th AUV, $\mathbf{s}_i(t) \in \mathbb{R}^3$ denotes its velocity relative to $\{I\}$, expressed in body-fixed coordinates, and $\boldsymbol{\mathcal{R}}_i(t) \in SO(3)$ is the rotation matrix from $\{B_i\}$ to $\{I\}$, which satisfies $\dot{\boldsymbol{\mathcal{R}}}_i(t) = \boldsymbol{\mathcal{R}}_i(t)\boldsymbol{\mathcal{S}}(\boldsymbol{\omega}_i(t))$, where $\boldsymbol{\omega}_i(t) \in \mathbb{R}^3$ is the angular velocity of $\{B_i\}$, expressed in body-fixed coordinates of the i-th AUV, and $\boldsymbol{\mathcal{S}}(\boldsymbol{\omega})$ is the skew-symmetric matrix such that $\boldsymbol{\mathcal{S}}(\boldsymbol{\omega})\boldsymbol{x}$ is the cross product $\boldsymbol{\omega} \times \boldsymbol{x}$. It is assumed that an Attitude and Heading Reference System (AHRS) installed on-board each AUV provides measurements of both $\boldsymbol{\mathcal{R}}_i(t)$ and $\boldsymbol{\omega}_i(t)$. Finally, $\mathbf{a}_i(t) \in \mathbb{R}^3$ denotes a linear acceleration measurement provided by an accelerometer mounted on-board the AUV, and $\mathbf{g}_i(t) \in \mathbb{R}^3$ is the acceleration of gravity, expressed in body-fixed coordinates of the i-th AUV. Using the Lyapunov state transformation introduced in [2],

$$\mathbf{x}_i(t) := \begin{bmatrix} \mathbf{x}_i^1(t) \\ \mathbf{x}_i^2(t) \\ \mathbf{x}_i^3(t) \end{bmatrix} = \boldsymbol{\mathcal{T}}_i(t) \begin{bmatrix} \mathbf{p}_i(t) \\ \mathbf{s}_i(t) \\ \mathbf{g}_i(t) \end{bmatrix},$$

with

$$\boldsymbol{\mathcal{T}}_i(t) = \begin{bmatrix} \mathbf{I} & \mathbf{0} & \mathbf{0} \\ \mathbf{0} & \boldsymbol{\mathcal{R}}_i(t) & \mathbf{0} \\ \mathbf{0} & \mathbf{0} & \boldsymbol{\mathcal{R}}_i(t) \end{bmatrix} \in \mathbb{R}^{9\times 9}, \quad (14)$$

which preserves stability and observability properties [4], yields the LTI system

$$\begin{cases} \dot{\mathbf{x}}_i(t) = \mathbf{A}_{CT}\mathbf{x}_i(t) + \mathbf{B}_{CT}\mathbf{u}_i(t) \\ \mathbf{y}_i(t) = \mathbf{C}_{CT}\mathbf{x}_i(t) \end{cases}, \quad (15)$$

where $\mathbf{u}_i(t) := \boldsymbol{\mathcal{R}}_i(t)\mathbf{a}_i(t)$ is the input,

$$\mathbf{A}_{CT} = \begin{bmatrix} \mathbf{0} & \mathbf{I} & \mathbf{0} \\ \mathbf{0} & \mathbf{0} & \mathbf{I} \\ \mathbf{0} & \mathbf{0} & \mathbf{0} \end{bmatrix} \in \mathbb{R}^{9\times 9},\ \mathbf{B}_{CT} = \begin{bmatrix} \mathbf{0} \\ \mathbf{I} \\ \mathbf{0} \end{bmatrix} \in \mathbb{R}^{9\times 3},$$

and $\mathbf{C}_{CT} = \begin{bmatrix} \mathbf{I} & \mathbf{0} & \mathbf{0} \end{bmatrix} \in \mathbb{R}^{3\times 9}$.

To achieve a discrete-time model of the dynamics, suppose that the inertial position measurements are obtained with a constant sampling rate, with corresponding period T, and assume that the measurements from the AHRS and the accelerometer are obtained with a much faster sampling rate. Then, the system (15) can be described by the discrete-time LTI system (7), with

$$\begin{cases} \mathbf{A}_L = e^{\mathbf{A}_{CD}T} \\ \mathbf{B}_L = \mathbf{I}_9 \\ \mathbf{C}_L = \mathbf{C}_{CD} \end{cases}$$

and

$$\mathbf{u}_i(k) = \int_0^T e^{\mathbf{A}_{CD}(T-\tau)}\mathbf{B}_{CD}\mathbf{u}_i(t_k + \tau)d\tau,$$

in which t_k denotes the sampling instant of sample k.

Regarding the second case, i.e., when the AUV has access to relative position measurements and receives position estimates from the corresponding vehicles, a similar procedure

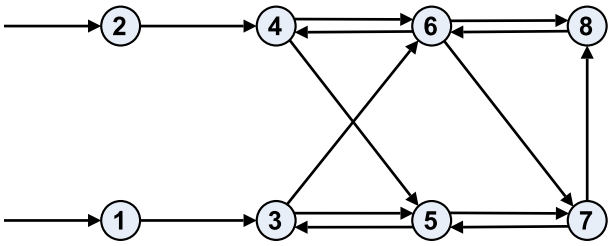

Fig. 1. Measurement graph for the formation considered in the simulations

can be carried out, yielding the system

$$\begin{cases} \dot{\mathbf{x}}_i(t) = \mathbf{A}_{CT}\mathbf{x}_i(t) + \mathbf{B}_{CT}\mathbf{u}_i(t) \\ \mathbf{y}_i(t) = \mathbf{C}^i_{CT}\Delta\mathbf{x}_i(t) \end{cases},$$

where $\mathbf{A}_{CT}$ and $\mathbf{B}_{CT}$ are defined as in the previous case, and $\mathbf{C}^i_{CT} = \mathbf{I}_{\nu_i} \otimes \mathbf{C}_{CT} \in \mathbb{R}^{3\nu_i \times 9\nu_i}$. The equivalent discrete-time model can be described by (9), with $\mathbf{A}_L$, $\mathbf{B}_L$, and $\mathbf{u}_i(k)$ defined as in (15), and $\mathbf{C}_i = \mathbf{C}^i_{CT}$.

A. Filter implementation

Following the previous discussion, it is straightforward to design local state observers following (2) and (3) or (5), depending on the available measurements. The local observers are then implemented in the body-fixed coordinate space of each respective vehicle. To do so, consider for the first case (inertial measurements) the following continuous-discrete representation: denoting the state estimate by $\hat{\mathbf{x}}_i(t) \in \mathbb{R}^9$, its update between samples of the output follows

$$\dot{\hat{\mathbf{x}}}_i(t) = \mathbf{A}_{CT}\hat{\mathbf{x}}_i(t) + \mathbf{B}_{CT}\mathbf{u}_i(t).$$

Then, when the output sample k is obtained at time t_k, update the state following

$$\hat{\mathbf{x}}_i(t_k^+) = \hat{\mathbf{x}}_i(t_k) + \mathbf{K}_i(\mathbf{y}_i(t_k) - \mathbf{C}_L\hat{\mathbf{x}}_i(t_k)).$$

Finally, invert the Lyapunov state transformation (14) by defining new state estimates $\hat{\mathbf{z}}_i(t) = \boldsymbol{\mathcal{T}}_i^{\mathsf{T}}(t)\hat{\mathbf{x}}_i(t)$. The update between samples of the output becomes

$$\dot{\hat{\mathbf{z}}}_i(t) = \mathbf{A}_i(t)\hat{\mathbf{z}}_i(t) + \mathbf{B}_{CT}\mathbf{a}_i(t),$$

with

$$\mathbf{A}_i(t) = \begin{bmatrix} \mathbf{0} & \boldsymbol{\mathcal{R}}_i(t) & \mathbf{0} \\ \mathbf{0} & -\boldsymbol{\mathcal{S}}(\boldsymbol{\omega}_i(t)) & \mathbf{I} \\ \mathbf{0} & \mathbf{0} & -\boldsymbol{\mathcal{S}}(\boldsymbol{\omega}_i(t)) \end{bmatrix} \in \mathbb{R}^{9\times 9}.$$

When an output sample is available, update the state estimate following

$$\hat{\mathbf{z}}_i(t_k^+) = \hat{\mathbf{z}}_i(t_k) + \boldsymbol{\mathcal{T}}_i^{\mathsf{T}}(t_k)\mathbf{K}_i(\mathbf{y}_i(t_k) - \mathbf{C}_L\hat{\mathbf{z}}_i(t_k)).$$

The same procedure can be carried out for the AUVs with relative measurements, yielding a similar continuous-discrete formulation.

B. Gain computation

Before computing the observer gains, both the measurement topology of the formation and the sensor noise need to be defined. In the simulations that were carried out, a formation composed of 8 AUVs was considered, and its measurement graph is depicted in Fig. 1. The positions measurements were sampled with constant period $T = 1\ (s)$.

Regarding sensor noise, all the measurements were corrupted by additive, uncorrelated, zero-mean white Gaussian noise, with appropriate standard deviations given the equipment that would usually provide those measurements:

- Inertial position measurements - 0.1 m;
- Relative position measurements - 0.2 m;
- Linear acceleration - 0.01 m/s^2;
- Angular velocity - $0.05\,^\circ$/s;
- Attitude, parametrized by Euler angles - $0.03\,^\circ$ for the roll and pitch, $0.3\,^\circ$ for the yaw.

The noise covariance matrices $\mathbf{Q}$ and $\mathbf{R}$ used for obtaining the observer gains were computed accordingly.

To provide a comparison term, observer gains were computed using the two methods introduced in [17] and adapted to the discrete-time case in [18]. The first method consists in computing the observer gains locally for each vehicle using pole placement. The second method provides improved observer gains computed through H_2 norm minimization. To initialize the finite-horizon algorithm, a sequence of estimation error covariances was computed using the aforementioned locally computed gains. The result of the optimization process is shown in Fig. 2, which depicts the evolution of the trace of $\mathbf{P}(k|k)$ for the locally computed gains as well as the set of observer gains obtained with the finite-horizon method. As it can be seen, the proposed solution was able to achieve a significant improvement in performance, and clearly achieved steady-state behavior. The projected steady-state performance for each method is shown in Table II.

TABLE II
PROJECTED PERFORMANCE FOR THE THREE COMPETING SOLUTIONS

	Locally computed	Finite-horizon	H2 norm
$\mathrm{tr}(\mathbf{P}_\infty)$	0.620	0.395	0.431

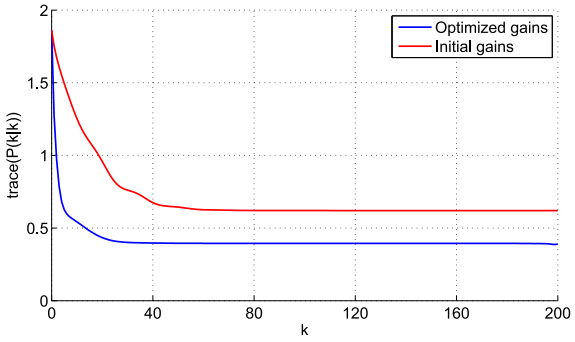

Fig. 2. Evolution of the estimation error covariance for both methods

C. Performance comparison

The initial positions of the agents and the trajectory followed by the formation are depicted in Fig. 3. The initial evolution and steady-state behavior of the norm of the total estimation error, defined as the vector composed of all estimation error variables in the formation, are depicted in Figs. 4 and 5, respectively. As it can be seen, for all three competing solutions the error converges to the vicinity of zero after an initial transient caused by the large error in

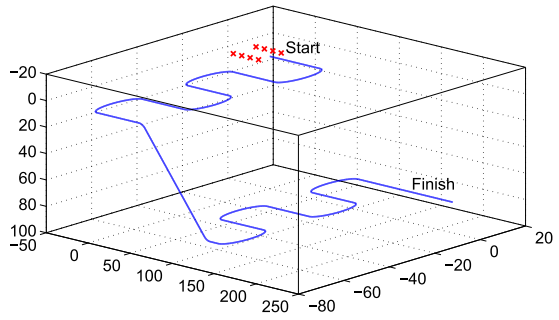

Fig. 3. Initial positions of the AUVs and trajectory

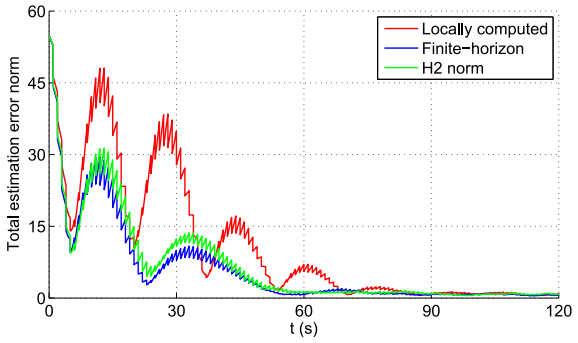

Fig. 4. Initial evolution of the norm of the total estimation error

the initial estimates, and remains there over the course of the simulation. To supplement the graphical data, Table III depicts the sum of the steady-state variance of all estimation error variables in the formation. To compute these variances, only the corrected state estimates were taken into account. As it can be seen, the gains obtained with the finite-horizon algorithm outperform the two other solutions, as was expected from the projected performance in Table II.

VI. Conclusions

This paper addressed the problem of distributed state estimation in a multi-vehicle framework. In the scenario envisioned in this work, each vehicle aims to estimate its own state by implementing a local state observer which relies on locally available measurements and limited communication with other vehicles in the vicinity. The dynamics of the problem were formulated as a more general discrete-time Kalman filtering problem with a sparsity constraint on the gain and, based on this formulation, a method for computation of steady-state observer gains for arbitrary fixed measurement topologies was introduced. The proposed method consists in the optimization of the time-varying distributed Kalman filter over a finite time window to approximate steady-state behavior and compute well-performing steady-state observer gains. To assess the performance of the proposed solution, simulation results were detailed for the practical case of a formation of AUVs that clearly illustrate the improvement over the two existing methods used for comparison.

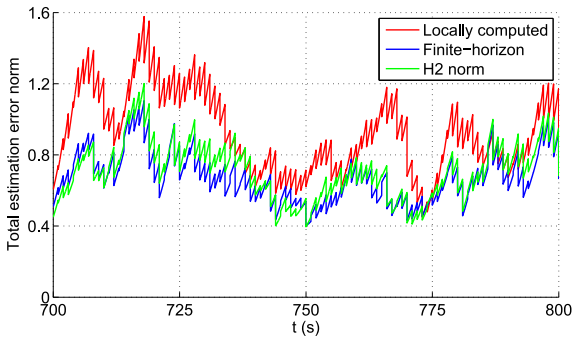

Fig. 5. Detailed view of the norm of the steady-state estimation error

TABLE III
Steady-state performance for the three competing solutions

	Locally computed	Finite-horizon	H2 norm
$\sum \sigma^2$	0.565	0.374	0.405

References

[1] BDO Anderson and J. B. Moore. *Optimal filtering*. Courier Dover Publications, 2012.

[2] P. Batista, C. Silvestre, and P. Oliveira. Position and Velocity Optimal Sensor-based Navigation Filters for UAVs. In *Proceedings of the 2009 American Control Conference*, pages 5404–5409, Saint Louis, USA, June 2009.

[3] J.G. Bender. An overview of systems studies of automated highway systems. *IEEE Transactions on Vehicular Technology*, 40(1):82–99, February 1991.

[4] R. W. Brockett. *Finite Dimensional Linear Systems*. Wiley and Sons, 1970.

[5] T. B. Curtin, J. G. Bellingham, and D. Webb. Autonomous Oceanographic Sampling Networks. *Oceanography*, 6:86–94, 1993.

[6] C.M. Fransson and B. Lennartson. Low order multicriteria H_∞ design via bilinear matrix inequalities. In *Proceedings of the 42nd IEEE Conference on Decision and Control*, volume 5, pages 5161–5167, December 2003.

[7] F. Giulietti, L. Pollini, and M. Innocenti. Autonomous formation flight. *IEEE Control Systems Magazine*, 20(6):34–44, December 2000.

[8] A.J. Healey. Application of formation control for multi-vehicle robotic minesweeping. In *Proceedings of the 40th IEEE Conference on Decision and Control*, volume 2, pages 1497–1502, 2001.

[9] K. Liu, H. B. Lim, E. Frazzoli, H. Ji, and V. C. S. Lee. Improving positioning accuracy using gps pseudorange measurements for cooperative vehicular localization. *IEEE Transactions on Vehicular Technology*, 63(6):2544–2556, July 2014.

[10] Magdi S Mahmoud. *Decentralized control and filtering in interconnected dynamical systems*. CRC Press, 2010.

[11] F. Pasqualetti, R. Carli, and F. Bullo. Distributed estimation via iterative projections with application to power network monitoring. *Automatica*, 48(5):747 – 758, 2012.

[12] S. Quintero, M. Ludkovski, and J. P. Hespanha. Stochastic Optimal Coordination of Small UAVs for Target Tracking using Regression-based Dynamic Programming. *Journal of Intelligent & Robotic Systems*, 82(1):135–162, 2016.

[13] M. Rokowitz. On Information Structures, Convexity, and Linear Optimality. In *Proceedings of the 47th IEEE Conference on Decision and Control*, pages 1642–1647, Cancun, Mexico, December 2008.

[14] Jeff Shamma. *Cooperative Control of Distributed Multi-Agent Systems*. John Wiley & Sons, 2008.

[15] R. Sousa, P. Oliveira, and T. Gaspar. Joint Positioning and Navigation Aiding Systems for Multiple Underwater Robots. In *8th IFAC Conference on Manoeuvring and Control of Marine Craft-MCMC 2009*, pages 167–172, Guaruja, Brazil, September 2009.

[16] H. G. Tanner and D. K. Christodoulakis. Decentralized cooperative control of heterogeneous vehicle groups. *Robotics and Autonomous Systems*, 55(11), November 2007.

[17] D. Viegas, P. Batista, P. Oliveira, and C. Silvestre. Decentralized H_2 observers for position and velocity estimation in vehicle formations with fixed topologies. *Systems & Control Letters*, 61(3):443–453, March 2012.

[18] D. Viegas, P. Batista, P. Oliveira, and C. Silvestre. Gas decentralized navigation filters in a continuous-discrete fixed topology framework. In *Control & Automation (MED), 2013 21st Mediterranean Conference on*, pages 1286–1291. IEEE, 2013.

[19] Y. Yuan and H. G. Tanner. Sensor Graphs for guaranteed cooperative localization performance. *Control and Intelligent Systems*, 2010.